WAVE-PLASMA INTERACTIONS INVOLVING INTENSE RUNAWAY ELECTRON STREAMS

H. M. SKARSGARD, A. R. STRILCHUK and W. W. ZUZAK

University of Saskatchewan, Saskatoon, Saskatchewan, Canada

A strong electric field applied to a toroidal plasma in a magnetic field produces an intense runaway electron stream, consisting of essentially all the electrons of the plasma. However, after an initial normal acceleration, the electrons experience less-than-normal acceleration followed by deceleration and disruption of the stream. Intense bursts of microwave radiation occur during the current pulse. The observed time of disruption is compared with the value expected from the theory of the two-stream instability. Reasonably good agreement is found. Average ion and electron temperatures have been determined.

1. Introduction

Many investigations have been carried out recently on the wave-plasma interactions which occur when a low density electron stream passes through a relatively high density plasma. Agreement between experimental observations and some of the theoretical predictions indicates that these phenomena are beginning to be understood. In this paper we report an investigation of wave-plasma interactions involving an intense stream of runaway electrons. This stream consists of essentially all the electrons of the plasma and is produced by applying a strong electric field to a plasma in a torus. Preliminary work /1/ showed that the runaway electrons do not continue to accelerate in a normal manner and that the stream is disrupted soon after its formation. Measurements of the current and the electron concentration /2/ show the behaviour of the stream from the time of its formation until its disruption. The observed behaviour is compared with the predictions of the theory of the two-stream instability. Spectroscopic measurements provide some information on the manner in which the plasma oscillations affect the thermal energy of the plasma.

2. Experimental System

The interior of the glass torus (Fig. 1) is coated with a thin layer of graphite giving a resistance of 100 ohms per cm length around the chamber. Argon and xenon gases have been used at pressures from 10^{-4} to 10^{-3} Torr. An azimuthal magnetic field (B_Φ) is provided by 18 solenoidal coils (not shown in Fig. 1) uniformly spaced around the torus. One pulsed operation of the system begins with the application of this magnetic field. When the magnetic field is near its peak value the plasma is formed by inductively coupling a 3 Mc/sec rf field into the chamber to ionize the gas. The rf duration is of the order of a few hundred microseconds. The amplitude decays with time so that adjustment of the rf duration controls the plasma concentration at the moment the rf is turned off and the accelerating electric field E^b is applied. The accelerating field is provided by an air-cored betatron winding /3/ connected in series with two 5-μF capacitor banks. The circuit gives an oscillatory electric field at a frequency of 116 kc/sec. Most of the observations are made during the first quarter-cycle ($\approx 2\,\mu$ sec). Plasma switches /4/ in the betatron circuit have a

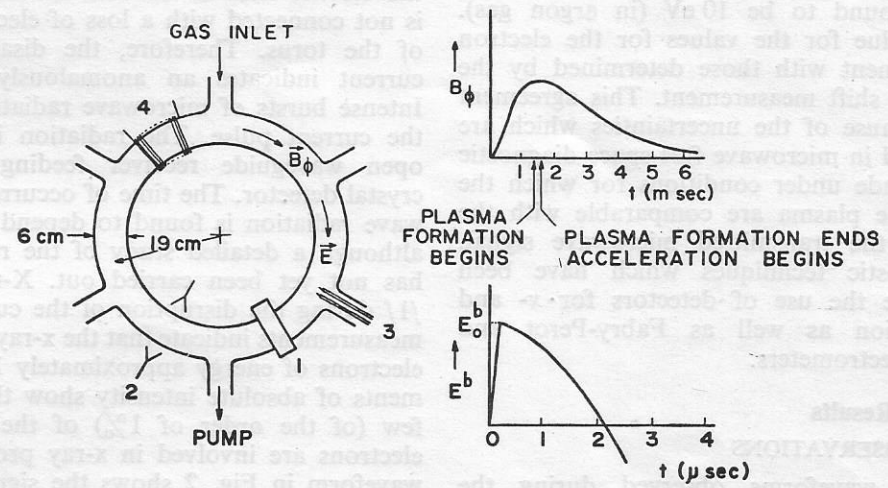

Fig. 1. Experimental system. 1 — Rogowski coil; 2 — microwave open waveguide transmitting and receiving antennae; 3 — double electrostatic probe; 4 — diamagnetic coil.

closing time of the order of 0.2 μ sec. The accelerating field becomes strong compared with the critical runaway field /5/ shortly after the switches are triggered.

A Rogowski coil is used to measure the current flowing around the torus. The electric field is measured by a pickup loop placed close to the betatron winding. This gives the form of the betatron electric field; the absolute magnitude is obtained by a calibration procedure which makes use of a pickup loop inserted around the interior of the torus. The electron concentration and temperature at the beginning of the acceleration phase (end of rf pulse) are determined by measurements with a microwave interferometer, a movable double electrostatic probe and a diamagnetic coil. Windows in the graphite coating of the torus, adjacent to the open waveguide (3 Gc/sec) transmitting and receiving antennae, facilitate the microwave transmission through the plasma and the measurement of the phase shift introduced by the plasma. Assuming a constant electron temperature across the torus as indicated by early afterglow measurements /6/ the saturation probe current during the rf discharge, measured by an ac method /7/, determines the relative electron density (approximately a cosine shape) across the torus. (Because of difficulty in measuring the "equivalent resistance" of the plasma during the rf discharge it was not possible to determine the electron temperature with the probes.) A 50-turn shielded coil wound around the torus is used to measure the diamagnetic signal corresponding to ionization of the gas during the application of the rf field /8/; this measurement determines the product $(nT_{e\perp})$ where n is the electron concentration and $T_{e\perp}$ is the temperature corresponding to the electron motion perpendicular to the magnetic field B_Φ. If we assume that the electron energy is equally distributed among the three degrees of freedom (i. e. a Maxwellian velocity distribution) during the rf discharge and substitute for the density the electron temperature the saturation probe current then leads to value determined by the microwave interferometer then the electron temperature is found to be 10 eV (in argon gas). By using this value for the values for the electron density in agreement with those determined by the microwave phase shift measurement. This agreement is important because of the uncertainties which are generally involved in microwave free-space diagnostic measurements made under conditions for which the dimensions of the plasma are comparable with the wave length of the transmitted microwave signal.

Other diagnostic techniques which have been employed include the use of detectors for x- and microwave-radiation as well as Fabry-Perot and prism optical spectrometers.

3. Experimental Results

3.1. GENERAL OBSERVATIONS

The various waveforms observed during the formation and disruption of the runaway electron stream are shown in Fig. 2. The results were obtained using argon at a pressure of approximately 0.4×10^{-3} Torr. The current reaches a maximum at approximately 0.4 μ sec and then falls to practically zero

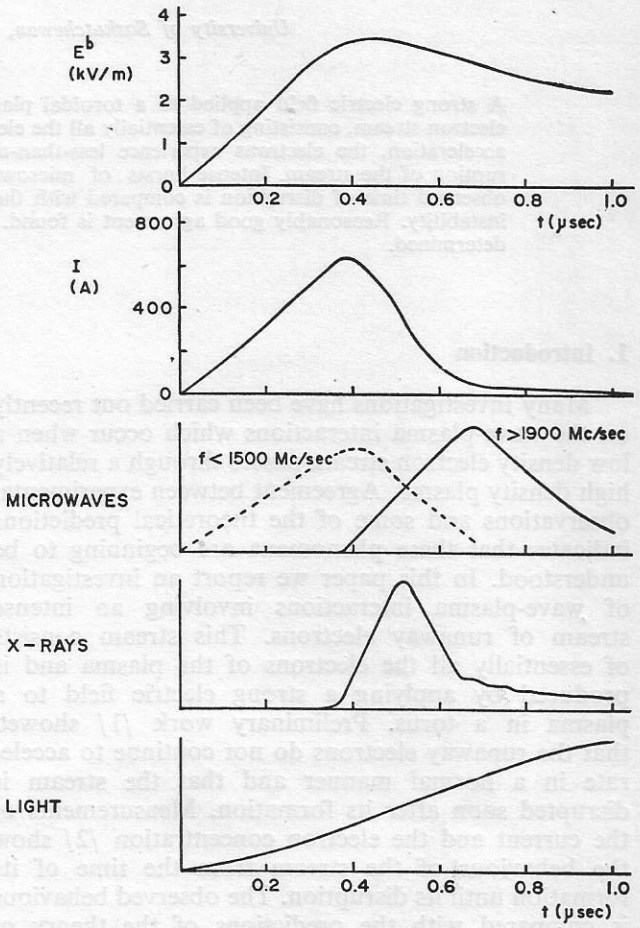

Fig. 2. Observed waveforms.

even though the electric field is still large. The measured electron concentration is closely constant during the first microsecond after the application of the electric field E^b so that the decrease in current is not connected with a loss of electrons to the walls of the torus. Therefore, the disappearance of the current indicates an anomalously high resistance. Intense bursts of microwave radiation appear during the current pulse. The radiation is detected by an open waveguide receiver feeding directly into a crystal detector. The time of occurrence of the microwave radiation is found to depend on the frequency although a detailed study of the radiation spectrum has not yet been carried out. X-rays are observed /1/ during the disruption of the current. Absorption measurements indicate that the x-rays are produced by electrons of energy approximately 100 keV; measurements of absolute intensity show that only relatively few (of the order of 1%) of the total number of electrons are involved in x-ray production. The last waveform in Fig. 2 shows the signal from a photomultiplier placed in the focal plane of a quartz prism spectrometer. The waveform was generally the same

for all of the more intense optical emissions — which always originated from singly-ionized atoms.

3.2. ELECTRON STREAM BEHAVIOUR

From a knowledge of the current and the electron concentration, the average drift velocity around the torus $[\bar{v}(t)]_{\mathrm{Obs}}$ can be determined. (Since the electron density is nearly constant over the duration of the current pulse, the average drift velocity has the same time variation as the current). From the measured electric field E^b, corrected for the self-field associated with the observed rate of change of current, the actual electric field E can be determined as well as the velocity $[v(t)]_{N.A.}$ which this field would produce if the acceleration were normal. Fig. 3 shows the ratio $F(t) = d/dt\,[\bar{v}(t)]_{\mathrm{Obs}}/d/dt\,[v(t)]_{N.A.}$ for three different values of azimuthal magnetic field B_Φ. In each case the plasma concentration at the center of the chamber was 1.5×10^{11} cm^{-3} and the line density corresponded to $\nu = 0.49$ (ν is the number of electrons in a slice of the stream of thickness equal to one classical electron radius r_0; ν/r_0 is the number of electrons per unit length around the torus).

The average kinetic energy of the electron drift motion around the torus $\bar{W}_D(t)$ reaches a value of 1 to 2 keV at the peak current. Fig. 4 shows the ratio of $\bar{W}_D(t)$ to the total energy $W_T(t) = (\nu/r_0)^{-1} \times \int^t E\,I\,dt$ supplied by the electric field.

It is evident from Figs. 3 and 4 that the stream behaviour is not dependent on the strength of the magnetic field. The values of $F(t)$ and $\bar{W}_D(t)/W_T(t)$ become less reliable as $t \to 0$ because of the decreasing signal-to-noise ratio in the measurements of I and E^b. However, it is clear that these ratios are approximately unity initially and decrease with time.

Considering all of the experimental observations, we arrive at the following conclusions. The electrons accelerate initially in a normal manner and then after a time of approximately 0.1 μ sec, they experience less-than-normal acceleration followed by deceleration and disruption of the stream. As evidenced by the burst of microwave radiation this behaviour is presumably due to the onset of plasma oscillations which grow at the expense of the energy of drift motion and lead to the anomalous resistance observed. During the disruption of the stream a relatively small fraction of the electrons continue to be accelerated to high energies and produce x-rays when they strike the chamber walls.

Anomalously high resistance and the emission of x- and microwave-radiation have been observed in other toroidal plasma experiments /9, 10/. The detailed behaviour of the runaway electron stream from the moment of application of the accelerating field has not been reported previously. This behaviour can be compared with the theory of the two-stream instability (section 4).

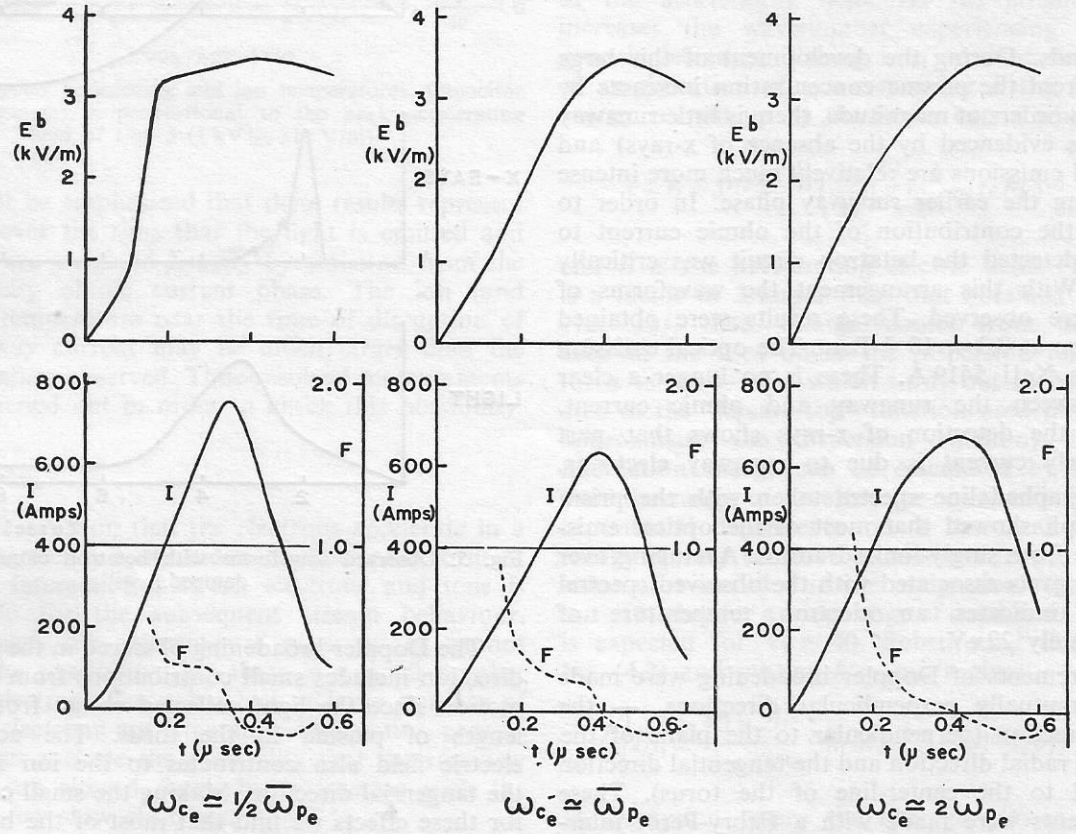

Fig. 3. Ratio F of the observed and normal acceleration for different magnetic fields. $\omega_{ce} = e B\Phi/m$ is the electron cyclotron frequency. ω_{pe} is the average electron plasma frequency.

3.3. SPECTROSCOPIC MEASUREMENTS

The spectroscopic measurements which have been made so far are not time-resolved but represent an average over the duration of the optical emission. The ringing betatron circuit, as it is operated to produce the waveforms of Fig. 2, gives relatively large current oscillations in the plasma after a few

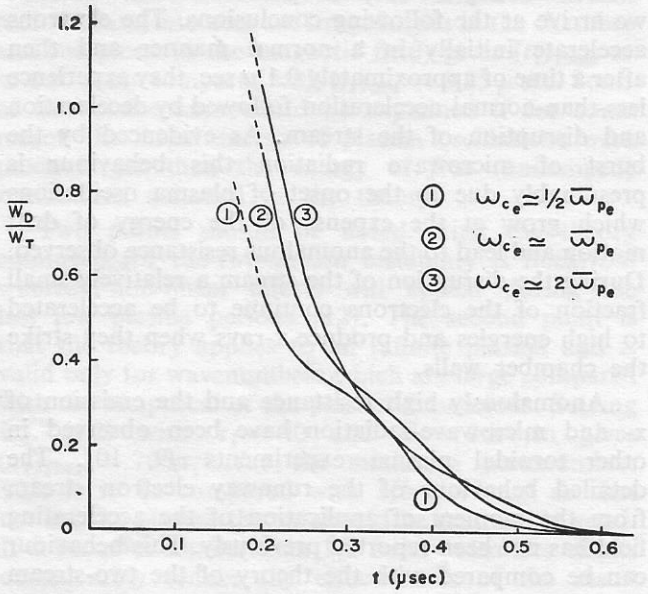

Fig. 4. Ratio of the average electron drift energy and the total energy supplied.

microseconds. During the development of this large ohmic current the plasma concentration increases by one or two orders of magnitude, there is little runaway current (as evidenced by the absence of x-rays) and the optical emissions are relatively much more intense than during the earlier runaway phase. In order to minimize the contribution of the ohmic current to the light detected the betatron circuit was critically damped. With this arrangement the waveforms of Fig. 5 were observed. These results were obtained using xenon at 0.3×10^{-3} Torr. The optical emission detected is XeII 5419 Å. There is no longer a clear break between the runaway and ohmic current. However, the detection of x-rays shows that part of the early current is due to runaway electrons.

Photographed line spectra taken with the prism spectrograph showed that most of the optical emissions were from singly-ionized atoms. Averaging over the upper levels associated with the observed spectral emissions indicates an electron temperature of approximately 22 eV.

Measurements of Doppler broadening were made in three mutually perpendicular directions, — the vertical direction (perpendicular to the plane of the torus), the radial direction and the tangential direction (tangential to the center-line of the torus). These measurements were made with a Fabry-Perot interferometer. Filters were used to isolate the spectral line of interest. The ring pattern was photographed and scanned with a microphotometer. The etalon employed was actually designed to have a high reflection coefficient in the 5900 Å region and gave a rather low finesse of 9 for the XeII 5419 Å emission. However, this was not serious since the Doppler broadening observed (Fig. 6) was comparatively large. The Doppler broadening observed in the radial and vertical directions was larger than in the tangential direction and cannot therefore be explained by the motion of ions in thermal equilibrium. It is possible that mass motion associated with diffusion and drift in the inhomogeneous magnetic field is responsible for part of the broadening in the radial and vertical directions although it has not been possible to give a quantitative explanation in terms of these effects /11/.

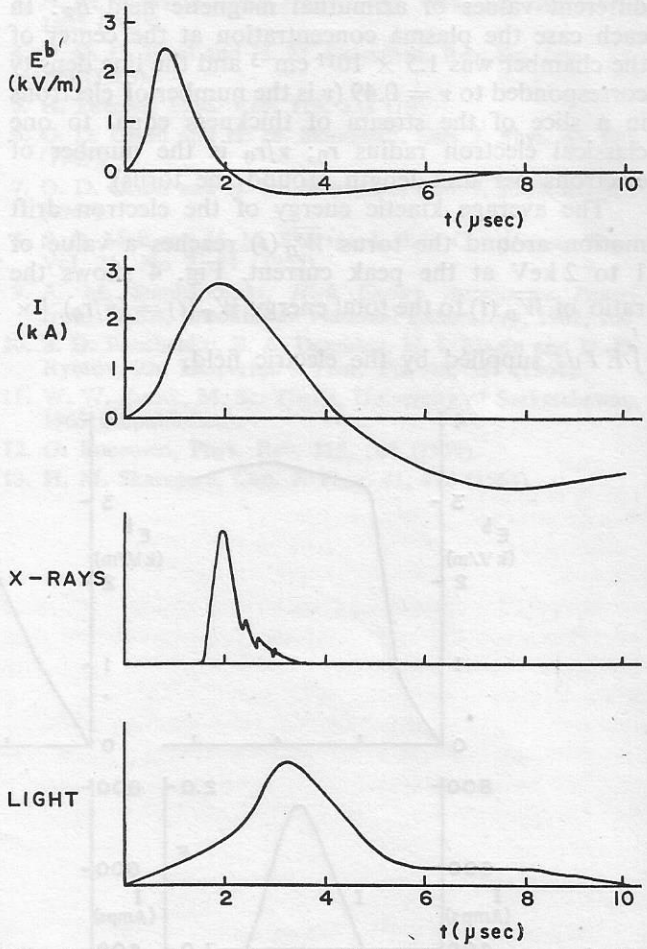

Fig. 5. Observed waveforms with betatron circuit critically damped.

The Doppler broadening observed in the tangential direction includes small contributions from the radial motion since the light collected comes from a finite length of plasma in the torus. The accelerating electric field also contributes to the ion motion in the tangential direction. Making the small corrections for these effects we find that most of the broadening observed in the tangential direction is due to some type of ion motion in the tangential direction. This

could be either thermal motion or collective (wave) motion or a combination of the two. If we assume it is entirely thermal motion this gives the ion temperatures shown in Fig. 6. The temperature increases with accelerating field. It is relatively independent of pressure and increases only slowly with magnetic field.

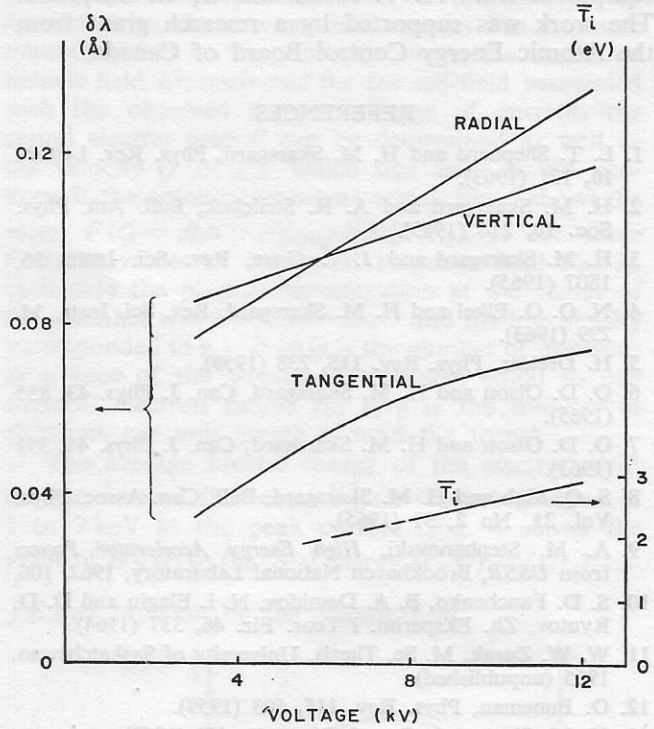

Fig. 6. Doppler broadening and ion temperatures. Capacitor voltage (abscissa) is proportional to the peak accelerating field of Fig. 5 (1 kV ≡ 310 V/m).

It must be emphasized that these results represent averages over the time that the light is emitted and therefore are weighted heavily by emission from the high density ohmic current phase. The ion (and electron) temperature near the time of disruption of the runaway current may be much larger than the average values observed. Time-resolved measurements will be carried out in order to check this possibility.

4. Discussion

The observation that the electrons accelerate in a normal manner initially indicates that some form of collective interaction between electrons and ions is responsible for the subsequent stream behaviour. Even though the experimental observations cannot exclude the possibility that there is a small number of slow electrons through which a large number of runaway electrons are streaming, momentum conservation does exclude the possibility that the runaway electrons are slowed down by interacting with the relatively few slow electrons.

This suggests that the disruption of the runaway electron stream is, at least in the early stages, a consequence of growing longitudinal plasma oscillations associated with the two-stream instability (electrons interacting with ions). Longitudinal oscillations should not depend strongly on the strength of the magnetic field — in agreement with experimental observations.

The experimentally observed time of disruption $(t_1)_{\mathrm{Obs}}$, defined as the time at which the kinetic energy of the streaming motion becomes just one-half of the total energy supplied, is approximately 0.25 μ sec (Fig. 4). It is found that $(t_1)_{\mathrm{Obs}}$ is not only independent of B_Φ but also independent of the peak accelerating electric field as determined by the capacitor voltage in the betatron circuit. These observations can be compared with the theory of the two-stream instability /12, 13/.

The maximum growth rate of the instability is /12/

$$\alpha_m = 3^{1/2}\, 2^{-4/3} \left(\frac{m}{M}\right)^{1/3} \omega_{pe}\,, \qquad (4.1)$$

where α_m is the imaginary part of the complex frequency ω, m and M are the electron and ion masses, ω_{pe} is the electron plasma frequency. Maximum growth occurs for $v = \omega_{pe}/k$, where v is the electron stream velocity and k is the wavenumber of the growing oscillation. The energy of oscillation is built up through amplification of free plasma oscillations initially present prior to the application of the accelerating field. As the stream velocity increases the wavenumber experiencing maximum growth decreases. Taking into account the duration of amplification of a wavenumber k the fluctuation energy is built up by the factor exp τ where

$$\tau = 6 \times 3^{1/2}\, 2^{-1/3} \left(\frac{m}{M}\right)^{2/3} \omega_{pe}^2\, m\,(eEk)^{-1} \qquad (4.2)$$

and E is the accelerating electric field. (This result is a factor of 2 larger than that obtained previously /12, 13/. The change comes from taking into account the area under the dispersion relation plot for α vs $(kv - \omega_{pe})$ which turns out to be twice the area of the "square top" function used previously to approximate the dispersion relation). The total fluctuation energy can be calculated by integrating over the range of k-values (or τ-values). Due to the exponential dependence on τ the total fluctuation energy is very sensitive to changes in the maximum value of τ included in the integration. Thus it turns out /13/ that for a wide range of conditions disruption is expected for $\tau_1 \simeq 40$. Substituting this value in Eq. (4.2) and putting $k = \omega_{pe}/v$ gives

$$(v/E)_1 \simeq \frac{40 \times 2^{1/3}}{6 \times 3^{1/2}} (m/M)^{-2/3}\, (2\, v^{1/2}\, c/b)\, e/m \qquad (4.3)$$

at disruption where the average plasma frequency $\bar{\omega}_{pe} = 2\, v^{1/2}\, c/b$ has been used; c is the speed of light and b is the radius of the stream. Taking

$v = (e/m)\int_0^t E(t)\,dt$ shows that for any given form of $E(t)$ the expected time of disruption $(t_1)_{\text{Theor}}$ is independent of the magnitude of the electric field — in agreement with experimental observations. Substituting the actual electric field (betatron plus self-inductance field), $m/M = 1.37 \times 10^{-5}$ (for argon), $\nu = 0.49$ and $b = 0.024$ m (the effective stream radius taking into account irregularities in the chamber and bumpiness in the magnetic field) gives $(t_1)_{\text{Theor}} \simeq \simeq 0.67\ \mu$ sec compared with $(t_1)_{\text{Obs}} = 0.25\ \mu$ sec. Some of this discrepancy could be explained if for some reason the initial energy of plasma oscillations were much larger than the energy of free (undamped) oscillations assumed in the theory.

Two points should be noted. First the theory employed for the two-stream instability is linearized whereas non-linear effects will appear during the last few plasma periods /12/. The second point is that the theory applies to an infinite plasma and is valid only for wavenumbers which are large compared with the reciprocal of the plasma dimensions. Solving Eq. (4.2) with $\tau_1 = 40$ and $E_1 = 3$ kV/m gives $(k_1)_{\text{Theor}} = 70\ \text{m}^{-1}$ for the minimum wavenumber. This is to be compared with $1/b \simeq 40\ \text{m}^{-1}$ so that the infinite plasma theory should be reasonably good. If k becomes smaller than $1/b$ finite beam size effects considerably reduce the effectiveness of the instability /13/.

Future work will include a study of the microwave radiation and a measurement of the time of disruption for different plasma densities. This should determine more conclusively whether or not the two-stream instability is responsible for the behaviour of the runaway electron stream.

Acknowledgement

The authors gratefully acknowledge the technical assistance of W. Rovers and the loan of spectroscopic equipment from A. V. Jones and G. G. Shepherd. The work was supported by a research grant from the Atomic Energy Control Board of Canada.

REFERENCES

1. L. T. Shepherd and H. M. Skarsgard, Phys. Rev. Letters **10,** 121 (1963).
2. H. M. Skarsgard and A. R. Strilchuk, Bull. Am. Phys. Soc. **10,** 214 (1965).
3. H. M. Skarsgard and J. V. Gore, Rev. Sci. Instr. **36,** 1807 (1965).
4. N. O. O. Eikel and H. M. Skarsgard, Rev. Sci. Instr. **34,** 299 (1963).
5. H. Dreicer, Phys. Rev. **115,** 238 (1959).
6. O. D. Olson and H. M. Skarsgard, Can. J. Phys. **43,** 855 (1965).
7. O. D. Olson and H. M. Skarsgard, Can. J. Phys. **41,** 391 (1963).
8. S. Q. Mah and H. M. Skarsgard, Bull. Can. Assoc. Phys. Vol. 21, No 2, 51 (1965).
9. A. M. Stephanovski, *High Energy Accelerator Papers* from *USSR*, Brookhaven National Laboratory, 1962, 106.
10. S. D. Fanchenko, B. A. Demidov, N. I. Elagin and D. D. Ryutov, Zh. Eksperim. i Teor. Fiz. **46,** 337 (1964).
11. W. W. Zuzak, M. Sc. Thesis, University of Saskatchewan, 1965 (unpublished).
12. O. Buneman, Phys. Rev. **115,** 503 (1959).
13. H. M. Skarsgard, Can. J. Phys. **41,** 450 (1963).